THERMOMECHANICAL PROPERTIES OF CVI-PROCESSED Si-B-C BASED CARBIDES AS DERIVED FROM THE BEHAVIOR OF CARBON FIBER-REINFORCED MICROCOMPOSITES

A. Michaux, C. Sauder, G. Camus and R. Pailler

Laboratoire des Composites Thermostructuraux, UMR 5801 (CNRS-SNECMA-CEA-UB1)
3 allée de la Boétie, 33600 Pessac, France

ABSTRACT

The thermomechanical behavior (longitudinal Young's modulus and thermal expansion coefficient, rupture strength) of different ceramic phases in the Si-B-C system have been determined from room temperature up to 1200°C using a specific high temperature testing apparatus. Viscoplasticity is observed at 1200°C and is related to the amorphous boron containing phases. Experimental results have been used to compute thermal residual stresses in model systems using a layered matrix. Results have evidenced an important step-like distribution of the axial stresses which could favourably influence the deviation of matrix cracking inside a composite.

1. INTRODUCTION

A new concept of self-healing and layered CVI-processed ceramic matrix has been developed in order to increase the oxidation resistance of continuous fiber-reinforced composites [1]. Improving the efficiency of such matrices while avoiding many empirical trial tests has made necessary the setting up of numerical models aimed at predicting some thermochemical and thermomechanical properties of the layered composite materials. In this respect, a first important step consists in obtaining a precise knowledge of the basic properties of each material constitutive of the layered matrix. Previous studies have shown that materials in the Si-B-C system are efficient to get a good oxidation protection in a large temperature range, i.e. from 450° to 1500°C [2]. Since most of the published works only deal with the improvement of the oxidation resistance of ceramic matrix composites, no thermomechanical data are available regarding CVI-processed Si-B-C based ceramics, at the exception of silicon carbide. These data are however essential for the modelling of the internal stress distribution resulting from processing.

The present study is thus aimed at establishing some thermomechanical properties of various Si-B-C based carbides, i.e. boron carbide B_4C, materials of the Si-B-C system with different boron contents and silicon carbide SiC.

An original method, based on thermomechanical tests performed on carbon fiber/ceramic matrix microcomposites, has been used to determine the Young's modulus, rupture strength and thermal expansion coefficient of each constituent of the layered matrix as a function of temperature. These properties have been established by an inverse method using a specific device previously developed at LCTS [3, 4], which allows to determine longitudinal Young's modulus and longitudinal thermal expansion coefficient of coated and uncoated carbon fibers, from room temperature up to 1200°C, under inert atmosphere.

2. EXPERIMENTAL PROCEDURE

2.1. Materials

The carbon fiber used for the processing of the microcomposites is the commercial XNO5 fiber (from Nippon Graphite Fiber), whose characteristics are well known and reported in table 1. This fiber has been selected because of its low Young's modulus, its regular and circular cross-section (easily measured by laser diffraction) and its nearly isotropic characteristics. Such characteristics allow (i) to emphasize the part played by the matrix in the global behavior of the microcomposites and (ii) to minimize the calculation uncertainties related to the fiber properties.

"**Table 1.** Characteristics of the pitch-based XNO5 carbon fiber (Nippon Graphite Fiber)."

Mean diameter (µm) †	10
Young's modulus (GPa) ††	52 (± 2)
Stress to failure (MPa) with L_0 = 50 mm ††	1060 (± 175)
Resistivity (Ω.m) ††	26 (± 1)
Conductivity ($W.m^{-1}.K^{-1}$) †	4
Longitudinal thermal expansion coefficient ($.10^{-6}$ °C^{-1}) ††	0,87 at 22°C
	$[8,47.10^{-10}.T^3 - 3,33.10^{-6}.T^2 + 4,95.10^{-3}.T + 7,61.10^{-1}]$ from 22°C up to 1600°C (T in °C)
Density ††	1,61

† from supplier ; †† after Sauder [4]

The various ceramic matrices were deposited, by chemical vapor infiltration [5], on carbon fibers previously mounted on graphite racks. Besides a common CVI-SiC, two different boron carbides, referred to as $B_4C(1)$ and $B_4C(2)$ were obtained through the use of two different processing conditions, resulting in two slightly different chemical compositions, see table 2. Similarly, two materials of the Si-B-C system were also processed, denoted as Si-B-C(1) and Si-B-C(2) in table 2, where Si-B-C(1) stands for the material with the higher silicon content. Chemical composition of the different ceramic coatings indicated in table 2 have been determined using ESCA analysis.

"**Table 2.** Chemical composition of the different matrices (ESCA analysis)."

	Si (% atomique)	**B (% atomique)**	**C (% atomique)**
$B_4C(1)$	-	a	b
$B_4C(2)$	-	a - 4 %	b + 4%
Si-B-C(1)	x	y	z
Si-B-C(2)	x - 31%	y + 35%	z - 4%

X-ray, Raman spectroscopy and TEM analysis have also been performed on all the deposits in order to determine their microstructural organization. Results have shown that, whereas silicon carbide appears to be crystallized (cubic symmetry), all the other deposits present an amorphous structure. The Raman analysis (figure 1) clearly showed that there was neither free silicon nor free carbon present in the silicon carbide and in the Si-B-C(2) material. Conversely, there was very few free carbon in the boron carbides and in the Si-B-C(1) material.

Coating thicknesses and related matrix contents of the microcomposites are reported in table 3. All the coatings proved to be reasonnably regular in thickness along the gauge length of the microcomposites.

"Table 3. Characteristics of the microcomposites for the different matrices."

	$B_4C(1)$	**$B_4C(2)$**	**Si-B-C(1)**	**Si-B-C(2)**	**SiC**
Deposit thickness (µm)	2,9 (± 0,1)	2,6 (± 0,1)	5 (± 0,7)	4,5 (± 0,7)	6,9 (± 0,6)
Matrix volume ratio (average) (%)	58	56	72	71	81

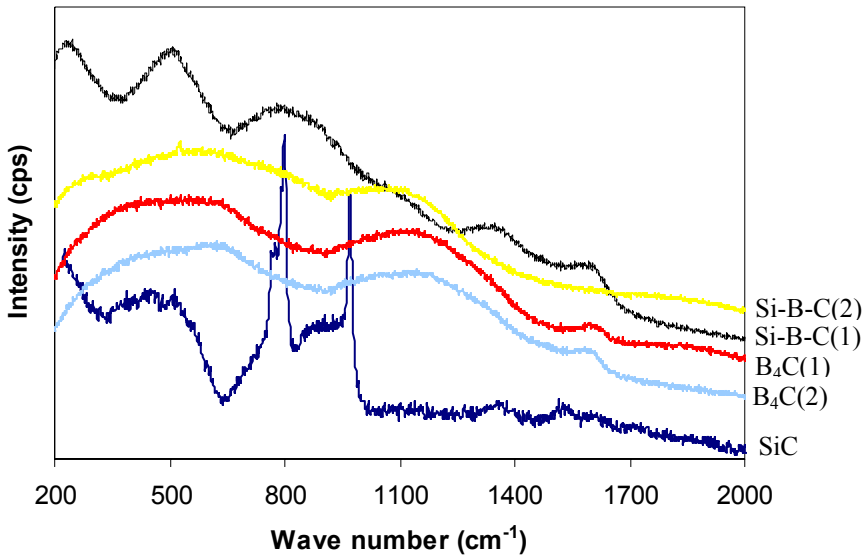

"**Fig. 1.** Raman spectra of the different deposits."

2.2. Thermomechanical testing

Tensile tests were performed from room temperature up to 1200°C under secondary vacuum (<10^{-3} Pa) on microcomposites with a gauge length of 50 mm, using a specific device described elsewhere [3,4] and schematically drawn in figure 2.

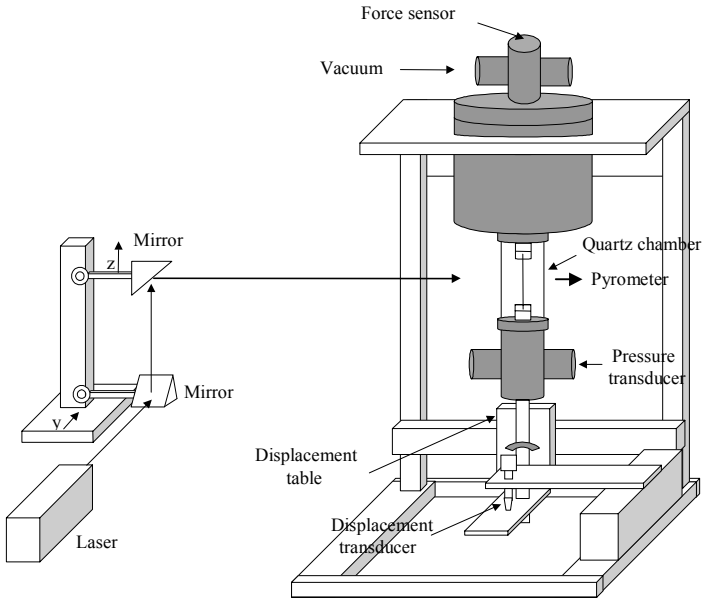

"**Fig. 2.** Schematic diagram of the high temperature fiber testing apparatus."

Samples were held between two graphite grips using a carbon-based cement (C34 from Ucar). Tests were performed up to rupture at a strain rate of 1%.min^{-1}. Strain measurements were derived from grip displacement by using a compliance calibration technique that allows deformation of the load frame to be taken into account [6]. Regarding high temperature characterisations and in order to avoid possible microstructural changes occuring during the tests, samples were maintained 30 minutes prior to testing (i) at the testing temperature in the case of tensile tests and (ii) at 1200°C in the case of thermal expansion measurements. These

last measurements were performed by applying and maintaining constant during sample testing a very low stress onto the microcomposites. The displacement which had to be applied thus balanced the longitudinal expansion of the sample induced by heating. Finally, it should be mentionned that computations of temperature distributions evidenced negligible gradients in the samples [6].
Young's modulus and thermal expansion coefficient of the various carbides were derived from the results of thermomechanical tests performed on microcomposites, using the rule of mixtures as follows :

$$E_c = E_f.V_f + E_m.V_m \qquad \text{which leads to} \qquad \mathbf{E_m = \frac{E_c - E_f.V_f}{V_m}} \tag{1}$$

With E_c : microcomposite longitudinal Young's modulus
E_f : fiber Young's modulus V_f : fiber volume ratio
E_m : matrix Young's modulus V_m : matrix volume ratio

$$\alpha_c = \frac{E_m.V_m.\alpha_m + E_f.V_f.\alpha_f}{E_c} \qquad \text{which leads to} \qquad \mathbf{\alpha_m = \frac{\alpha_c.E_c - E_f.V_f.\alpha_f}{E_m.V_m}} \tag{2}$$

With α_c, α_f, α_m : thermal expansion coefficients of the microcomposite, fiber and matrix (respectively).

Calculations have shown that [6], in the present case of matrix dominated microcomposites, in terms of volume ratio as well as longitudinal Young's modulus, the rule of mixtures represents an accurate solution of the Hashin's two cylinders model [7]. This model is, besides, particularly well suited to the microcomposites used in the present study since it relies on the two basic hypothesis of (i) a perfect bonding between the fiber and the matrix and (ii) two coaxial cylinders with an infinite length. The interfacial bond is likely strong (and therefore close to "perfection") since (i) there was no interphase interposed between the fiber and the matrix and (ii) tensile tests revealed a brittle behavior without any fiber pullout. Moreover, no microcracks were evidenced in the various matrices after processing (linear behavior of the microcomposites).

3. RESULTS AND DISCUSSION

3.1. Tensile tests at room temperature

Mechanical characteristics of the different matrices derived from the tests performed in tension at room temperature are summarized in table 4, where E_m, σ_{Rm}, ε_{Rm} represent the Young's modulus, the stress to failure and the strain to failure of the matrix, respectively.

"**Table 4.** Mechanical characteristics at room temperature."

	B_4C(1)	**B_4C(2)**	**Si-B-C(1)**	**Si-B-C(2)**	**SiC**
Microcomposite failure stress (MPa)	594 (± 83)	656 (± 130)	568 (± 122)	636 (± 82)	497 (± 124)
E_m (GPa)	442 (± 16)	419 (± 23)	355 (± 16)	373 (± 15)	416 (± 12)
σ_{Rm} (MPa)	951 (± 133)	1022 (± 155)	748 (± 153)	853 (± 125)	595 (± 148)
ε_{Rm} (%)	0,21 (± 0,03)	0,25 (± 0,05)	0,21 (± 0,04)	0,23 (± 0,03)	0,14 (± 0,03)
m	8,4	7,9	5,5	8,1	4,6
σ_o (MPa)	553	553	360	521	278

Since all the microcomposites behaved in a brittle manner, a noticeable scattering of the failure stresses was always observed. Statistical distributions of strength datta were thus determined on batches of about 20 test specimens using the well-known Weibull's model [8]. Results of this model, plotted under a classical Weibull's diagram (figure 3), gave access to the Weibull modulus m and to the scale factor σ_o (for a fixed reference volume V_o of 1 mm^3). The Weibull modulus represents the degree of scattering of the fracture data.

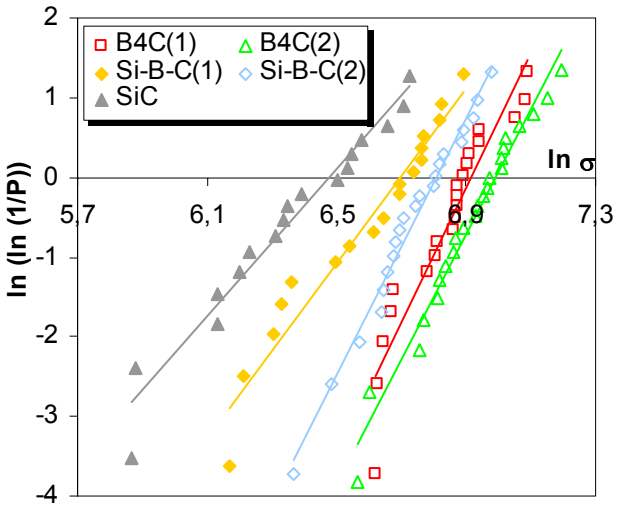

"**Fig. 3.** Weibull diagram for all the deposits."

High values of Weibull modulus are usually related to flaws which are homogeneous in size and well distributed in the material. Conversely, low values are related to flaws which are more scattered in their size and their distribution. It seems therefore that high boron containing materials ($B_4C(1)$, $B_4C(2)$ and Si-B-C(2)) have less critical flaws than high silicon containing materials (SiC, Si-B-C(1)).

In order to compare the stress to failure of various matrices, it is necessary to normalize the failure data reported in table 4, using the following formula :

$$\frac{\sigma_R'(V')}{\sigma_R(V)} = \left(\frac{V}{V'}\right)^{1/m} \qquad (3)$$

where V and V' are two different volumes under stress.
Results, shown in table 5 for a volume V' of 0.01 mm^3, indicate that amorphous phases have the higher stresses to failure.

"**Table 5.** Calculated room temperature failure properties of the ceramic matrices for a similar volume under stress."

	$B_4C(1)$	**$B_4C(2)$**	**Si-B-C(1)**	**Si-B-C(2)**	**SiC**
σ'_{Rm} (MPa)	900	933	776	865	687
ε'_{Rm} (%)	0,20	0,22	0,21	0,23	0,16

3.2. Tensile tests at high temperature

Figure 4 shows the evolution of the stress – strain curves of some of the different microcomposites investigated as a function of temperature. It should be mentionned that, in contrast with the previous analysis performed at room temperature, no statistical study has been made regarding the stress to failure values at high temperature. Consequently, no comparison could be made in terms of failure strengths. All the microcomposites exhibit a linear-elastic and brittle behaviour from room temperature to 1000°C. Over this temperature, i.e. at 1200°C, and except for the silicon carbide matrix microcomposite, all the other microcomposites exhibit a non-linear behavior. As there is obviously no possibility for multicracking of the matrix (the fiber volume ratio is too low), this non-linearity has to be attributed to a viscoplastic and/or a viscoelastic behavior. Such a time-dependent behavior can then be related to a time-dependent phenomenon present within the fiber, the interface or the matrix. The influence of the fiber should be excluded because (i) the matrix drives the microcomposite behavior and (ii) the C/SiC microcomposite remains linear at 1200°C. Interface sliding also seems to be excluded because of the likely strong bonding present between the fiber and the matrix. Consequently, it seems that the time-dependent behavior observed at 1200°C has to be related to the matrix and more precisely to the amorphous boron phases.

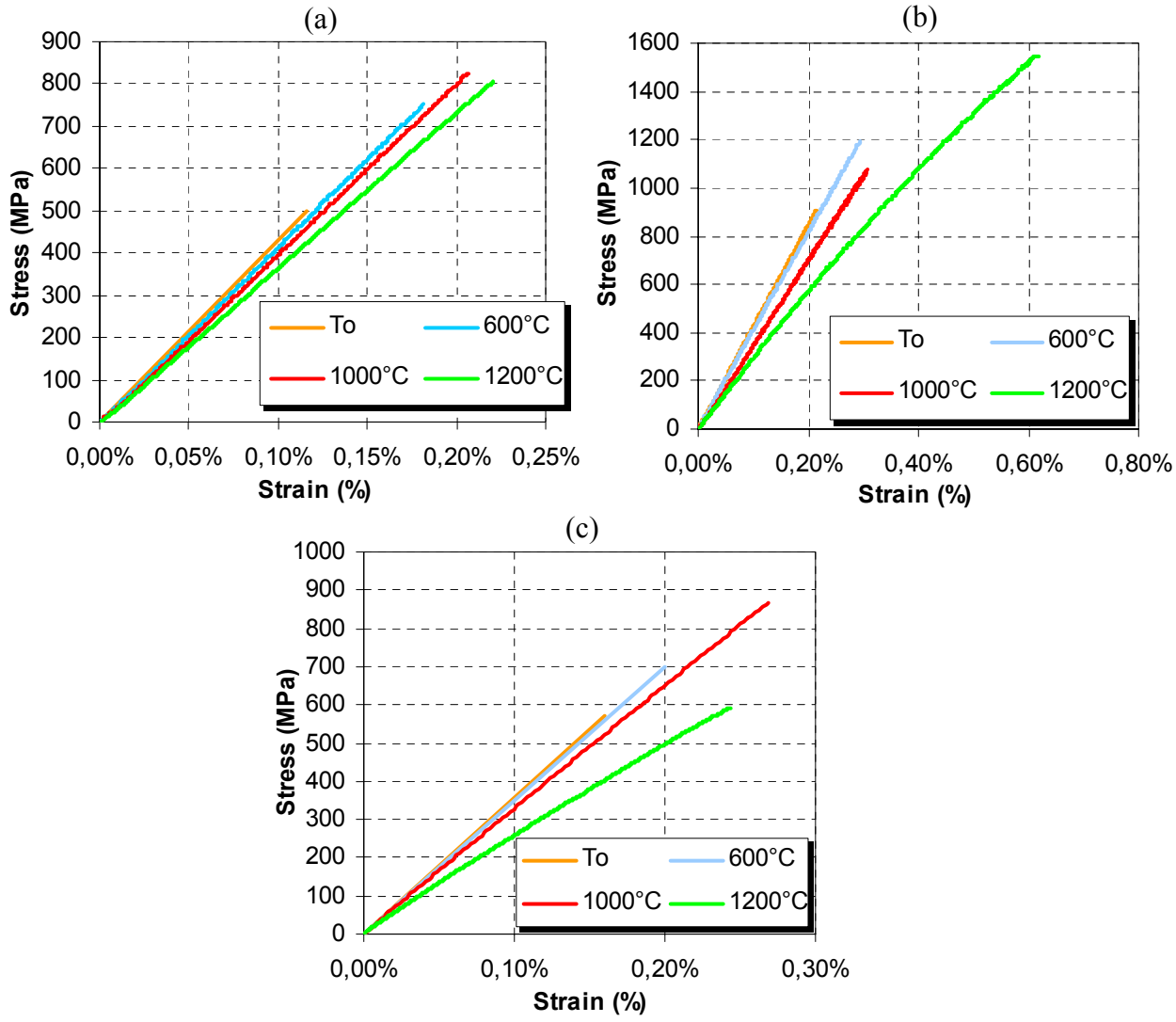

"**Fig. 4.** Evolution of stress - strain curves as a function of temperature for (a) silicon carbide, (b) boron carbide and (c) Si-B-C materials. "

Figure 5 displays, for each constituent, the evolution of the Young's modulus as a function of temperature. For all the deposits, the Young's modulus decreases in a constant manner with an increase in temperature, which has to be classically related to the progressive weakening of the chemical bonds.

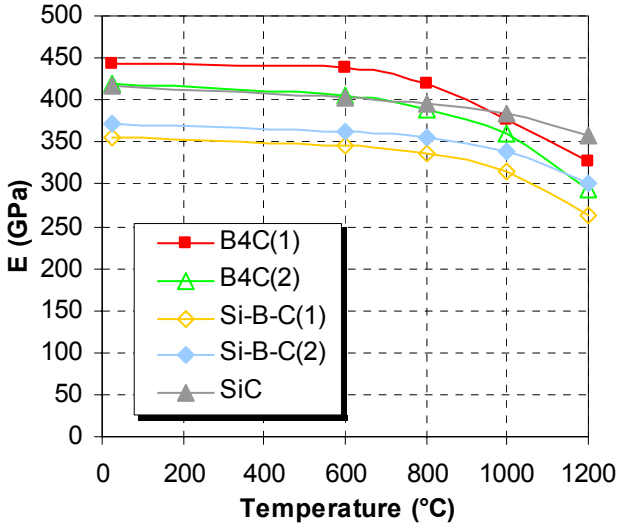

"**Fig. 5.** Young's modulus evolution as a function of temperature."

3.3. Thermal expansion coefficients

Figure 6 displays the evolution of the longitudinal thermal expansion coefficients of the various ceramic materials as a function of temperature. It may be seen that, for all the studied materials, these coefficients classically increase with temperature. However, it also appears that the thermal expansion coefficients of the boron-rich materials ($B_4C(1)$, $B_4C(2)$, Si-B-C(2)) are systematically higher than these of the silicon-rich materials (Si-B-C(1)), SiC). More investigations need to be performed in order to fully understand this last result.

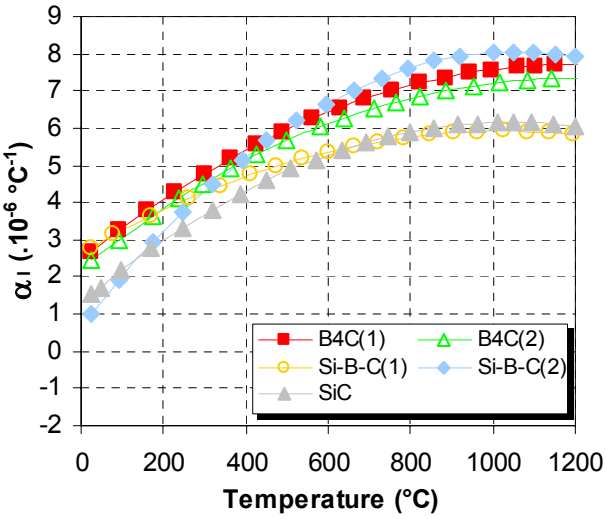

"**Fig. 6.** Evolution of the thermal expansion coefficient as a function of temperature."

4. THERMAL RESIDUAL STRESSES

Computations of thermal residual stresses have been performed on multilayered microcomposites, using the model developed by Warwick and Clyne [9], which constitutes an improvement of the one previously developed by Mikata and Taya [10]. This model is based on few basic hypothesis, largely similar to those used in the Hashin's two cylinders model, which are : (i) the microcomposite is supposed to be symmetric along its axis and infinite in length, (ii) interfacial bondings are supposed to be perfect, (iii) the different phases (of infinite thickness) are supposed to be isotropic or transversely isotropic (along z axis) and to behave in a linear elastic manner and (iv) the temperature inside the microcomposite is supposed to be uniform.

Calculations have taken into account previously experimentally determined evolutions of the thermomechanical characteristics of each constituent as a function of temperature. Regarding the isotropic ceramic materials (i.e. $B_4C(1)$, $B_4C(2)$, Si-B-C(1), Si-B-C(2) and SiC), the temperature-related evolution of their Young's modulus and thermal expansion coefficient was fitted by a polynomial regression of the experimental points (see figures 3 and 4). Conversely, since Poisson's ratio were not experimentally measured, their values were all set equal to 0.2, which is an average of the various values found in the literature. Calculations were performed on model microcomposite systems based on an ex-PAN carbon fiber. This kind of fiber has a markedly transverse isotropic symmetry and, since only the longitudinal thermoelastic coefficients were determined experimentally, the remaining coefficients were also taken from the literature.

Figure 7 displays an example of computed radial and axial residual stresses present in each layer of the multilayered matrix of a carbon fiber based microcomposite, in which the matrix is constituted by an alternation of boron-rich and silicon-rich layers. This diagram clearly shows that, at least for the thicknesses retained in this computation, the boron-rich and the silicon-rich layers are in a different state of axial tension or compression, which results in the presence of sudden rises (and drops) in the stress distribution. It may then be anticipated that this step-like stress distribution could favour microcrack deviation between each ceramic layer in the course of a mechanical test performed on a non-brittle composite. Of course, it would be interesting, in a future work, to tentatively compare experimental results with these calculations.

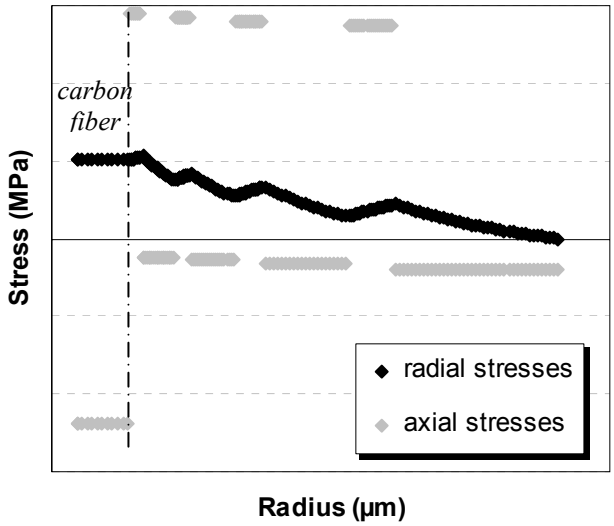

"**Fig. 7.** Stress distribution of a multilayered carbon fiber ceramic matrix microcomposite at room temperature."

5. CONCLUSIONS

An original method, based on thermomechanical tests performed on CVI-processed carbon fiber / Si-B-C based ceramic matrix microcomposites, has been used to determine the Young's modulus, rupture strength and thermal expansion coefficient of the various ceramic matrices as a function of temperature.

Results have allowed to point out two groups of materials as a function of their chemical composition. Boron-rich materials ($B_4C(1)$, $B_4C(2)$, Si-B-C(2)) have stresses to failure (at room temperature) higher than silicon-rich materials (Si-B-C(1)), SiC) as well as higher thermal expansion coefficients. It is thus very likely that this last family of materials has critical flaws more scattered in their size and their distribution.

Finally, the measured thermoelastic values of the ceramic materials have been used to calculate thermal residual stresses in model systems using a layered matrix. Results have evidenced an important step-like distribution of the axial stresses created by the alternation of ceramic matrix layers which could favorably influence the deviation of matrix cracking inside a composite. Further investigations need to be made in order to correlate these calculations with experimental results.

ACKNOWLEDGEMENTS

This work was supported by CNRS, Snecma Propulsion Solide and CEA. One of the author (A. M.) is grateful to CNRS and Snecma Propulsion Solide for support in the form of a research grant. The authors also wish to thank Pr E. Martin for his help in the computation of the thermal residual stresses model.

References

1. **Lamouroux, F., Bouillon, E., Cavalier, J.C., Spriet, P., Habarou, G.,** "An improved Long Life Duration CMC for Jet Aircraft Engine Applications", in *High Temperature Ceramic-Matrix Composites, W. Krenkel, R. Naslain, H. Schneider eds, Wiley-VCH, Weinheim (2001), 783-788.*
2. **Goujard, S., Vandenbulcke, L., Tawil, H.,** "The oxidation behaviour of two- and three-dimensionnal C/SiC thermostructural materials protected by chemical-vapour-deposition polylayers coatings", *J Mater Sci,* ***29*** *(1994), 6212-6220.*
3. **Sauder, C., Lamon, J., Pailler, R.,** "Thermomechanical properties of carbon fibers at high temperatures (up to 2000°C)", *Compos Sci Technol,* ***62*** *(2002), 499-504.*
4. **Sauder, C., Lamon, J., Pailler, R.,** "The tensile behavior of carbon fibers at high temperatures up to 2400°C", *Carbon (in press).*
5. **Naslain, R., Langlais, F., Fedou, R.,** "The CVI-processing of ceramic matrix composites", *J. Phys-Paris, C5,* ***50*** *(1989), 191-207.*
6. **Michaux, A.,** "Amélioration de la durée de vie de composites à matrice céramique à renfort carbone", *PhD thesis, University of Bordeaux I (2003).*
7. **Hashin, Z.,** "Analysis of properties of fiber composites with anisotropic constituents", *ASME J Appl Mech,* ***46*** *(1979), 543-550.*
8. **Lissart, N., Lamon, J.,** "Statistical analysis of failure of SiC fibres in the presence of bimodal flaw populations", *J Mater Sci,* ***32*** *(1997), 6107-6117.*
9. **Warwick, C.M.** and **Clyne, T.W.,** "Development of composite coaxial cylinder stress analysis model and its application to SiC monofilament systems", *J Mater Sci,* ***26*** *(1991), 3817-3827.*
10. **Mikata, Y.** and **Taya, M.,** "Stress field in a coated continuous fiber composite subjected to thermo-mechanical loadings", *J Compos Mater,* ***19*** *(1985), 554-578.*